10th U. S. National Combustion Meeting
Organized by the Eastern States Section of the Combustion Institute
April 23-26, 2017
College Park, Maryland

Effect of Distillate Fraction of Real Jet Fuel on Sooting Propensity – Part 1: Nascent Soot Formation in Premixed Stretch-Stabilized Flames

Chiara Saggese[1,], Ajay V. Singh[1], Joaquin Camacho[2], Hai Wang[1]*

[1]Mechanical Engineering Department, Stanford University, Stanford, CA 94304
[2]Mechanical Engineering Department, San Diego State University, San Diego, CA 92182
[*]Corresponding Author Email: csaggese@stanford.edu

Abstract: Real jet fuels are complex mixtures of many organic components, some of which are aromatic compounds. Towards the high-temperature end of the distillation curve, some of the aromatics may contain multiple rings. A trace amount of these high molecular weight species in the fuel would directly allow for soot nucleation in practical engines especially when the fuel is injected as a spray. This work aims to highlight the variation of the sooting propensity as a function of distillate fractions. Evolution of soot particle size distribution functions (PSDFs) is studied in a series of premixed stretch-stabilized ethylene-oxygen-nitrogen flames doped with Jet A or a certain distillate fraction. Mobility particle size distributions functions, soot volume fraction, and number density are determined by a Scanning Mobility Particle Sizer (SMPS). The results show that the tail end of the distillation curve can produce significantly more soot than the light molecular fraction and the not distilled jet fuel. The implication of the experimental finding on modeling soot formation from real jet fuel combustion will be discussed.

Keywords: Soot, premixed stretch-stabilized flame, jet fuel

1. Introduction

Jet A (POSF10325) is a common aviation fuel available in the United States. The fuel is comprised of thousands of hydrocarbon compounds [1], among which around 16 wt% are aromatic [2, 3]. The distillation curve of typical jet fuels give hints that are consistent with the existence of high molecular weight species in the fuel. Volatility information as derived from the measurement of the advanced distillation curve temperatures, along with the examination of the composition of each individual distillation fraction can be found in literature [2, 3]. The distillate fraction composition shows that towards the high-temperature end of the distillation curve some of the aromatics contain multiple rings, e.g., naphthalene, indane and tetraline [2, 3]. Knowing that multi-rings aromatics are precursors closer to soot formation [4], a trace amount of these high molecular weight species would allow for soot nucleation in a more direct manner in practical engines, especially when the fuel is injected as a liquid spray.

The aim of this work is to highlight the variation of the sooting propensity as a function of distillate fractions. In Part 1 of this work, the effect of distillate fractions on soot formation was

studied in a series of premixed stretch-stabilized ethylene-oxygen-nitrogen flames doped with Jet A or a certain distillate fraction, while in Part 2 is explored in non-premixed flames [5].

2. Experimental

Jet A was distilled into 8 distillate volume fractions (0-60%, 60-70%, 70-75%, 75-80%, 80-85%, 85-90%, 90-95% and 95-100% or residue) following the procedure described in literature [2, 3]. The obtained distillation curve is shown Fig. 1, along with the density measurement for each distillate fraction.

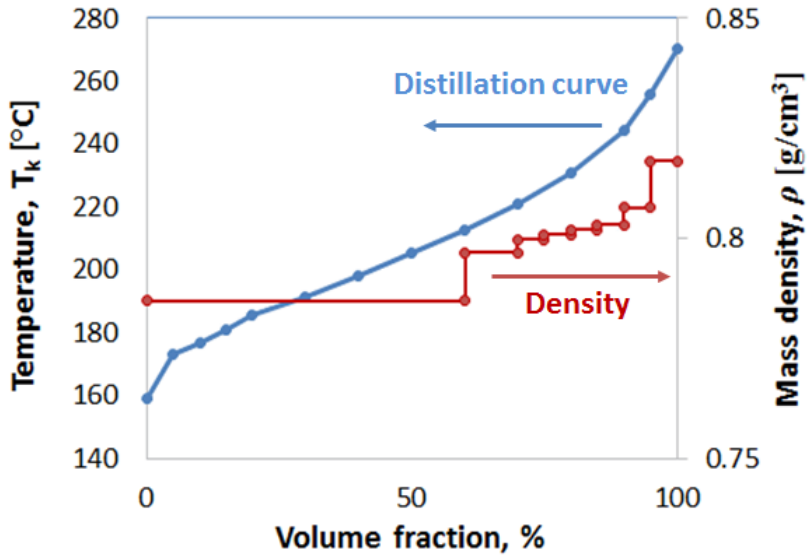

Figure 1: Representative distillation curve for Jet A and density of each volume distillate fraction, which have been measured as a part of the current work.

The heaviest fraction has an evaporation temperature higher than 270 °C. In comparison, the boiling points of naphthalene and phenanthrene are 218 °C and 332 °C. It is possible that even higher molecular weight species are present in the fuel in a dissolved form. Distillation did produce a solid residue at the end of the distillation process. Since the distillation setup was protected by a continuous purge of nitrogen, it is unlikely that the solid residue is the result of oxidation. The difference in density between the lightest fraction 0-60% and the residue corresponds to a derived molecular weight of 153.5 g/mol and 163.1 g/mol and to H/C ratio of 1.97 and 1.88, respectively.

The flame experimental setup, summarized in the left panel of Fig. 2, consists of a burner with an aerodynamically shaped nozzle, a stagnation surface/sampling probe assembly and a scanning mobility particle sizer (SMPS), identical to the one used in a previous work [6]. The aerodynamic shape of the burner nozzle body was designed to achieve plug flow at the burner exit (1.43 cm nozzle exit diameter). The distance between the burner nozzle and stagnation surface was held constant at 1.0 cm. The standing distance between the flame and stagnation surface/sampling probe was varied by changing the unburned gas flow rate. The flame is pseudo-one dimensional and amenable to numerical simulation using the OpenSMOKE++ code [7] and the HyChem model for

Jet A combustion [8, 9] with boundary conditions appropriate for the current stagnation flame problem.

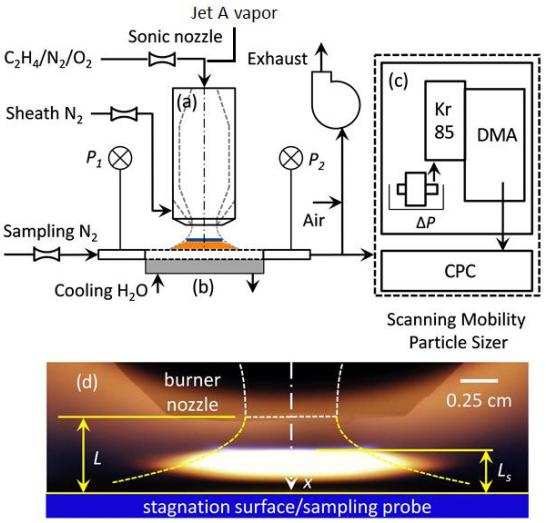

Flame	Fuel (ppm in mass)	$\Phi_{C2H4+JETA}$	Cold gas velocity[a], v_o (cm/s)
Jet A ($\rho_{o,liquid}$ = 0.803 g/cm^3, 158.6 g/mol)			
JetA-a	7262	2.18	50.3
JetA-b	7260	2.18	45.2
JetA-c	7252	2.18	39.7
0-60 light fraction ($\rho_{o,liquid}$ = 0.786 g/cm^3, 153.5 g/mol)			
0-60%JetA-a	7255	2.18	50.3
0-60%JetA-b	7269	2.18	45.2
0-60%JetA-c	7251	2.18	39.7
95-100 heavy fraction ($\rho_{o,liquid}$ = 0.817 g/cm^3, 163.1 g/mol)			
residue-a	7254	2.18	50.3
residue-b	7267	2.18	45.2
residue-c	7260	2.18	39.7

[a] STP condition (298 K, 1 atm)

Figure 2: Left panel: schematic showing various parts of the experimental setup. (a) Aerodynamically-shaped nozzle, (b) sampling probe/stagnation surface, (c) Scanning Mobility Particle Sizer, (d) A typical flame image; right panel: flame parameters.

Soot mobility size distributions were measured at the stagnation surface along the center axis of the flame. The stagnation surface is water-cooled. A micro-orifice (127 μm diameter, 125 μm wall thickness) embedded within the stagnation surface draws a flame sample continuously, which is quickly diluted by a flow of cold nitrogen thus quenching the reaction and preventing particle losses by coagulation. Soot PSDF is determined in terms of mobility diameter as measured by a Scanning Mobility Particle Sizer (SMPS). The gas temperature at the nozzle exit, T_n, is measured with an uncoated fine-wire (125 μm wire diameter) Pt-Rh thermocouple placed near the centerline of the flow. Similar to the BSS flame sampling technique [10], the stagnation surface also acts as a sampling probe. The temperature at the stagnation surface, T_s, is measured by a type-*R* thermocouple (0.2 cm wire diameter) placed flush with the surface such that the bead is exposed to the sample gas 1 cm away from the centerline of the flame. The gas temperature at the nozzle exit was determined to be T_n = 513 ±10 K, and the stagnation surface temperature is T_s = 368 ±25 K. The uncertainty values quoted here are one standard deviation across all flames studied.

A near-sooting ethylene-oxygen-nitrogen flame (12.2% C_2H_4, 17.8% O_2, 70% N_2, Φ = 2.06) was used as a host flame. Jet-A or a given distillate fraction was pre-vaporized before reaching the burner nozzle body and then ~7200 ppm in mass were doped into the unburned gas. PSDFs were determined for three series of flames, with different dopants: Jet A, the lightest distillate fraction (0-60%) and the heaviest distillate fraction (95-100% or residue). The unburned gas composition and cold gas velocity are summarized in the right panel of Fig. 2 for each series. The variation in the unburned gas velocity has the effect of changing the flame standoff distance by altering the kinematic balance between the local flame speed and the normal flow velocity immediately

upstream of the flame surface. The nitrogen sheath flow velocity matched to the cold gas velocity for each flame because the flame edges can be impacted for high sheath flow rates.

3. Results and Discussion

Axial velocity and temperature profiles computed for the flames doped with Jet A are shown in the left panel of Fig. 3. The maximum temperatures are 1885, 1899 and 1896 K for flames a, b and c, respectively. The preheat zone of the flame is not attached to the burner, which is typical for stretch-stabilized flames. Rather, the rise in temperature occurs where the local flow velocity approaches the laminar flame speed of the underlying mixture. The variation in the unburned gas velocity corresponds to changes in the global strain rate of the flame, which in turn causes the flame standing distance and the particle residence time to vary within each series of the flame. As an example, numerical solution of selected major and minor species of Flame Jet A-c is shown in the right panel Fig. 3.

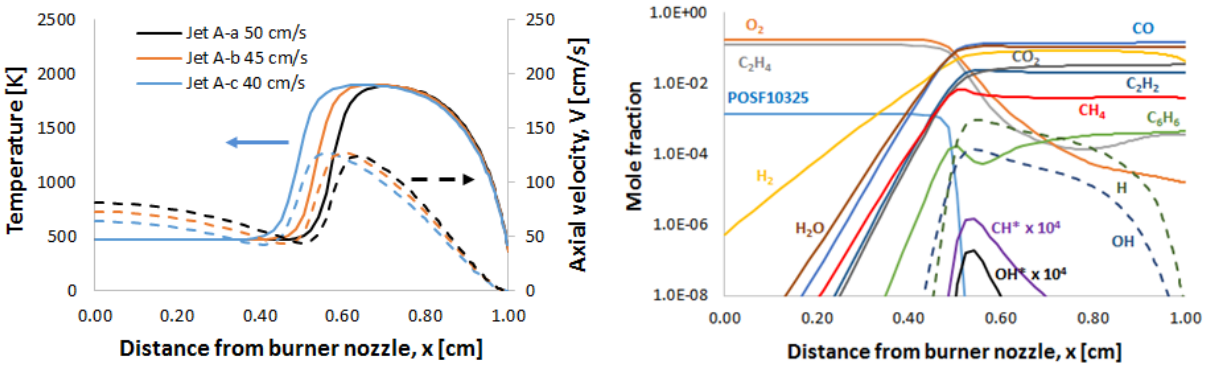

Figure 3: Left panel: profiles of temperature (solid lines) and velocity (dashed lines) for flames doped with Jet A; right panel: profiles of species mole fraction for the flame Jet A-c (see the table in Fig. 1).

The observed soot PSDFs are shown in Fig. 4, while the corresponding soot volume fraction is presented in Fig. 5. Under all equal conditions, the last 5 vol% of the heavy components (residue) produces three times more soot than the first 60 vol% of the light components. The particles measured are typically about 5 nm in mobility diameter and thus are small, incipient particles, showing that the nucleation mode is indeed sensitive to the distillate fractions of Jet A. Since the current study focuses on premixed flames in which the fuel must pass through the flame before it has a chance to nucleate and grow soot, the setup inherently suppress the effect of distillation fraction on soot nucleation and growth. This effect under the conditions of spray combustion may be even more significant.

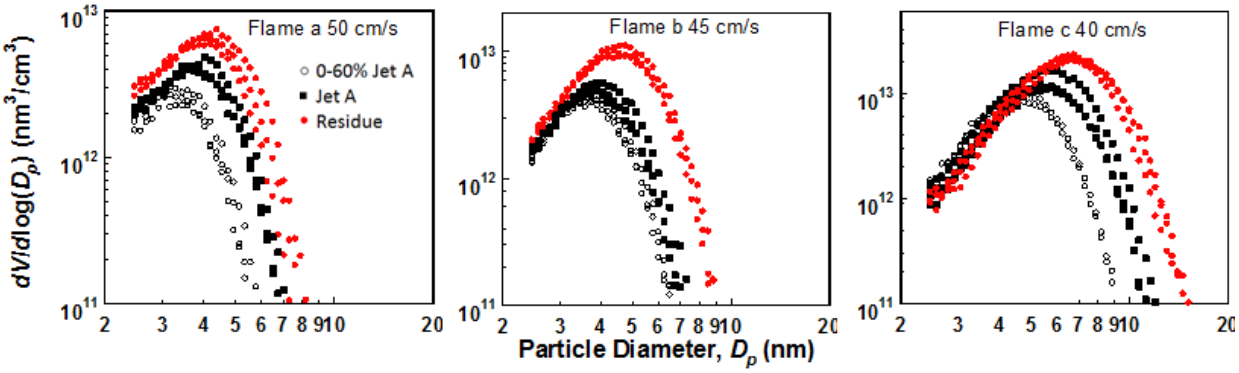

Figure 4: Mobility size distributions of a, b and c series of flames of Jet A as received (black squares), 0-60% Jet A (open circles) and residue (red circles).

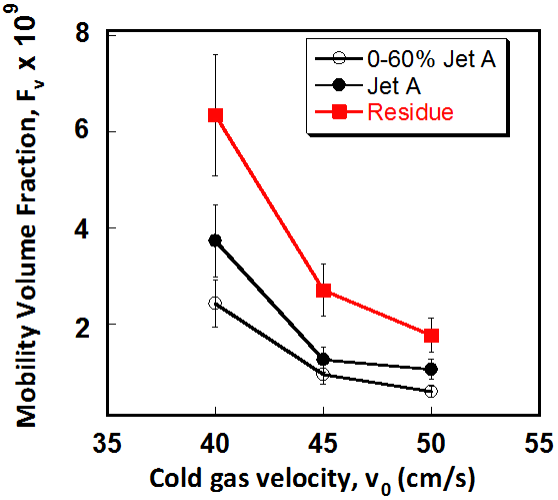

Figure 5: Mobility volume fraction of nascent soot measured at the stagnation surface in three series of 12.2% C_2H_4-17.8% O_2-70% N_2 host flames doped with 7200 ppm by mass of Jet A as received or its 0-60% and 95-100% distillate fractions.

The observation that soot formation is sensitive to the distillation fraction poses yet another challenge in modeling soot formation in real fuels, especially considering the possibility of preferential evaporation of the fuel from low-to-high molecular weights in spray combustion. Clearly, the surrogate fuel approach cannot account for the impact of preferential evaporation and its effect on soot formation.

4. Conclusions

Mobility size distribution functions of nascent soot were studied in a series of premixed stretch-stabilized ethylene-oxygen-nitrogen flames doped with Jet A as received or a certain distillate fraction of the same Jet A. The measurements show that components in the tail end of the distillation curve can produce significantly more soot than the light molecular fraction and the fuel as received. The results indicate that it remains challenging to model soot formation in practical

jet fuels using the surrogate fuel approach, especially when in real engines preferential evaporation during spray combustion can amplify the distillation fraction effect observed herein.

5. Acknowledgements

This research was supported by the National Aeronautics and Space Administration under agreement number 13-C-AJFE-SU-006.

6. References

[1] F.L. Dryer, Chemical kinetic and combustion characteristics of transportation fuels, Proc. Combust. Inst. 35 (2015) 117-144.

[2] T.M. Lovestead, J.L. Burger, N. Schneider, T.J. Bruno, Comprehensive Assessment of Composition and Thermochemical Variability by High Resolution GC/QToF-MS and the Advanced Distillation-Curve Method as a Basis of Comparison for Reference Fuel Development, Energy Fuels 30 (2016) 10029-10044.

[3] B.L. Smith, T.J. Bruno, Improvements in the measurement of distillation curves. 4. Application to the aviation turbine fuel Jet-A, Ind. Eng. Chem. Res. 46 (2007) 310-320.

[4] H. Wang, Formation of nascent soot and other condensed-phase materials in flames, Proc. Combust. Inst. 33 (2011) 41-67.

[5] X. Xue, C.-J. Sung, H. Wang, Effect of distillate fraction of real jet fuel on sooting propensity – part 2: soot formation in nonpremixed counterflow flames, 10th National Meeting on Combustion, College Park, Maryland, 2015.

[6] J. Camacho, A.V. Singh, W. Wang, R. Shan, E.K. Yapp, D. Chen, M. Kraft, H. Wang, Soot particle size distributions in premixed stretch-stabilized flat ethylene–oxygen–argon flames, Proc. Combust. Inst. 36 (2017) 1001-1009.

[7] A. Cuoci, A. Frassoldati, T. Faravelli, E. Ranzi, OpenSMOKE++: An object-oriented framework for the numerical modeling of reactive systems with detailed kinetic mechanisms, Comput. Phys. Commun. 192 (2015) 237-264.

[8] Xu, R., Wang, H., Hanson, R.K., Davidson, D.F., Bowman, C.T, Egolfopoulos F.N, "Evidence supporting a simplified approach to modeling high-temperature combustion chemistry," U.S. 10th National Combustion Meeting, 2017, Maryland.

[9] Xu, R., Chen, D., Wang, K., Tao, Y., Shao, J. K., Parise, T., Zhu, Y., Wang, S., Zhao, R., Lee, D. J., Egolfopoulos, F. N., Davidson, D. F., Hanson, R. K., Bowman, C. T., Wang, H. "HyChem model: Application to petroleum-derived jet fuels." U.S. 10th National Combustion Meeting, 2017, Maryland.

[10] A.D. Abid, J. Camacho, D.A. Sheen, H. Wang, Quantitative measurement of soot particle size distribution in premixed flames - The burner-stabilized stagnation flame approach, Combust. Flame 156 (2009) 1862-1870.